Apoptosis (2019) 24:837–848
https://doi.org/10.1007/s10495-019-01562-8

MAGI1 mediates tumor metastasis through c-Myb/miR-520h/MAGI1 signaling pathway in renal cell carcinoma

Wei Wang[1,2] · Yanhua Yang[3] · Xinyi Chen[4,5] · Shihong Shao[2] · Shasha Hu[2] · Tingguo Zhang[1,6]

Published online: 27 July 2019

Abstract

Renal cell carcinoma (RCC) is the third most common urological cancer with highly metastatic potential. MAGI1 plays an important role in stabilization of the adherens junctions and has been confirmed to suppress invasiveness and metastasis in multiple cancers in clinic. However, its expression and anti-metastatic ability in RCC are still unclear. In this study, we demonstrated that MAGI1 was markedly decreased in the RCC and indicated poor survival. Furthermore, we found that MAGI1 suppressed the invasion and migration of human RCC cells. Mechanistic investigations revealed that MAGI1 stabilized the PTEN/MAGI1/β-catenin complex to inhibit β-catenin signaling pathway. Moreover, MAGI1 was targeted by miR-520h which was transcriptionally activated by c-Myb. Collectively, our findings suggested that MAGI1mediated tumor metastasis through c-Myb/miR-520h/MAGI1 signaling pathway in RCC.

Keywords MAGI1 · Renal cell carcinoma · Metastasis · miR-520h · c-Myb

Introduction

Renal cell carcinoma (RCC) is the most common form and responsible for up to 85% of kidney cancer which accounts for nearly 400,000 new cancer diagnoses and 175,000 deaths worldwide annually [1, 2]. Approximately 21% of the patients present with synchronous distant metastasis at diagnosis and 20% of the patients get asynchronous metastatic disease or local recurrence after treatment of which about 90% develop within 5 years [3]. Although systemic therapy for metastatic renal cell carcinoma (mRCC) has greatly evolved over the last 15 years, metastasis still remains the main cause for RCC-associated mortality [4, 5].

Cell junctions are sites of intercellular adhesion that maintain the integrity of epithelial tissue and regulate signaling between cells [6]. As critical mediators of cell junctions, adherens junctions connect the actin cytoskeleton of adjacent cells [7]. Dysregulation of adherens junctions is a significant step in the acquisition of a mesenchymal phenotype by epithelial cells, so-called epithelial-mesenchymal transition (EMT), which promotes tumor transformation and metastasis [8]. Membrane-associated guanylate kinase with an inverted repeat member 1 (MAGI1), associates with the tight and adherens junctions, belongs to membrane-associated guanylate kinase (MAGUK) family [9]. MAGI1 is always disrupted in tumor progression and is associated with invasiveness and metastasis [10]. Previous reports have reported that MAGI1 can inhibit tumor invasion and metastasis by regulating PTEN in hepatocellular carcinoma [11], reducing Wnt/β-catenin signaling pathway in colorectal cancer [12] or blocking MAPK/ERK signaling pathway in gastric cancer [13]. However, little is known about the

Electronic supplementary material The online version of this article (https://doi.org/10.1007/s10495-019-01562-8) contains supplementary material, which is available to authorized users.

✉ Tingguo Zhang
ztguo@sdu.edu.cn

1 Department of Pathology, Qilu Hospital, Shandong University, Jinan, Shandong, China

2 Department of Pathology, The Affiliated Hospital of Qingdao University, Qingdao, Shandong, China

3 Department of Pathology, Qingdao Municipal Hospital, Qingdao, Shandong, China

4 Department of Pathology, Qingdao Central Hospital, Qingdao, Shandong, China

5 Department of Pathology, The Second Affiliated Hospital of Qingdao University Medical College, Qingdao, Shandong, China

6 Department of Pathology, School of Basic Medical Sciences, Shandong University, NO. 44, Wenhuaxi Road, Jinan, Shandong, China

effects of MAGI1 on RCC metastasis. Hence, the present study investigated whether MAGI1 regulates RCC metastasis and elucidate the underlying mechanism mediated by MAGI1 in RCC.

Materials and methods

Patients and tissue specimens

Human patient study cohort collected 73 pairs of RCC tumor tissues and corresponding adjacent normal tissues. All tissue samples were surgically removed and paraffin embedded or stored in liquid nitrogen in Shandong University Qilu Hospital from September 2015 to May 2018 with patients' consents and Research Ethics Committee of Qilu Hospital's approval. None of the patients received chemotherapy or radiotherapy before surgery. Clinical parameters including gender, age, tumor size, TNM stage, Fuhrman grade and histological type were collected. Detailed information is listed in Table 1.

Table 1 Relationship between MAGI1 expression and clinical pathological characteristics in RCC patients

	Count	MAGI1 expression		P value
		High	Low	
Gender				
Male	41	17	24	0.162
Female	32	12	20	
Age (years)				
< 60	38	18	20	0.432
≥ 60	35	21	14	
Tumor size (cm)				
< 4	13	8	5	0.175
≥ 4, < 7	21	10	11	
≥ 7	39	13	26	
TNM stage				
T1–T2	16	11	5	< 0.001
T3–T4	23	10	13	
M1	34	8	26	
Fuhrman grade				
I–II	30	19	11	< 0.001
III–IV	43	10	33	
RCC subtype				
ccRCC	57	27	30	0.187
pRCC	12	5	7	
chRCC	4	1	3	

TNM tumor/node/metastasis, *ccRCC* clear cell RCC, *pRCC* papillary RCC, *chRCC* chromophobe RCC

Cell line culture, construction and transfection assay

Renal cell lines, including 786-O, A-498, OS-RC-2, ACHN, Caki-1, SKRC39 and HK-2, were purchased from the Committee on Type Culture Collection of Chinese Academy of Sciences (Shanghai, China). A-498 and ACHN cell lines were cultured in EMEM and supplemented with 2 mM glutamine, 1% non-essential amino acids, 1 mM sodium pyruvate, 10% fetal bovine serum (FBS) (Gibco). Cells were maintained in a 37 °C and 5% CO_2 culture environment. Lentivirus containing pLVX- MAGI1-puro and pLVX-sh-MAGI1-puro were used to establish MAGI1-overexpression and MAGI1-knockdown cell lines and selected by puromycin. Short-interfering RNA (siRNA) against PTEN (si-PTEN), c-Myb (si–c-Myb), miR-520 mimics and negative control (si-NC) were synthesized by Sangon Biotech (Shanghai, China) and the sequences were show in Table S1. MiRNA mimics and siRNA transfection were conducted with PEIpro (Polyplus) according to the manufacturer's instructions.

RNA isolation and real-time quantitative PCR

Total RNA was extracted from frozen tumor specimens and cell lines using Trizol reagent (Invitrogen) and treated with DNase I (Invitrogen). The PrimeScript™ RT reagent Kit (RR037A, Takara) and SYBR™ Green PCR Master Mix (4368577, Applied Biosystems) were used to reverse transcript the complementary DNA and quantify, respectively. MiRNA was transcribed and quantified by All-in-One™ miRNA qRT-PCR Detection Kit (QP016, GeneCopoeia™). The quantitative real-time PCR was performed on Applied Biosystems™ 7500 Fast Dx Real-Time PCR system (Applied Biosystems) with specific primers (Table S1) following the instructions of manufacturer. GAPDH or U6 wass used as an endogenous control. Expression of miRNA and protein were normalized to U6 and GAPDH, respectively.

Immunohistochemistry staining

Immunohistochemistry staining was done on 4 μm-thick sections from paraffin embedded tissues. Sections were then submerged in boiling citrate buffer (pH 6.0) for antigen retrieval. Sections were dewaxed in xylene and rehydrated in gradient ethanol, followed by blocking of endogenous peroxidase activity in 3% H_2O_2 for 30 min. Ultra-Vision Protein Block (BD) was applied to block non-specific background staining. The tissue sections were immunostained with an anti-MAGI1 antibody (ab37543, Abcam) overnight at 4 °C. After washing thrice with PBS, the sections were incubated with horseradish peroxidase-conjugated (HRP) goat anti-rabbit IgG for 30 min, followed by reaction with diaminobenzidine (DAB) and counterstaining with Mayer's hematoxylin.

Western blot, co-immunoprecipitation and qPCR

Protein from cell lines were lysed using RIPA protein extraction reagent (Beyotime, Beijing) supplemented with a protease inhibitor cocktail (Roche) and PMSF (Roche). The protein concentration was measured by the Bio-Rad protein assay kit. Approximately 40 μg of protein extract was electrophoresed on a 10% SDS- polyacrylamide gel electrophoresis (SDS-PAGE) and then transferred onto 0.22 μm nitrocellulose membrane (Sigma) and incubated with primary antibody against MAGI1 (ab37543), E-cadherin (ab15148), Vimentin (ab45939), PTEN (ab170941), pAkt S473 (ab81283), Akt (ab8805), p-GSK-3β(Ser9) (ab75814), GSK-3β (ab227208), p-β-catenin (Ser33/77) (ab11350), β-catenin (ab32572), Cyclin-D1 (ab16663), c-Myc (ab32072), Survivin (ab76424) or GAPDH (ab128915) overnight at 4 °C. Then washed and incubated with secondary antibody goat anti-rabbit IgG H&L (HRP) (ab6721). The ECL chromogenic substrate was used to visualize the bands. For immunoprecipitation assay, the supernatant was incubated with anti-MAGI1(sc-100326) or anti-c-Myb (ab226470) at 4 °C for 2 h and protein A Sepharose CL-4B beads (GE) were incubated with the supernatant overnight at 4 °C. Then the beads were washed thrice with RIPA buffer. The bound proteins or DNA fragments were eluted with SDS-PAGE loading buffer. The bound proteins were used for western blot and were quantified by Quantity One software (Bio-Rad ChemiDoc XRS). GAPDH was used as a control. The DNA fragments were used as templates for quantitative RCR.

Immunofluorescence microscopy

Cells were cultured for 2 days in six-well plate and fixed in 4% paraformaldehyde for 20 min. Then cells were permeabilized with 0.1% Triton X-100 for 15 min, and blocked with 1% BSA for one hour. Cells were stained with primary antibody to β-catenin (ab32572) overnight at 4 °C. Cells were washed in PBS (pH 7.4), incubated with secondary antibody goat anti-rabbit IgG H&L (FITC) (ab6717). Nuclei were stained with DAPI (Sigma). The cells were visualized using a Nikon Eclipse E600 image analysis system.

Wound healing assay

2.5×10^5 MAGI1-overexpression and MAGI1-knockdown cell lines were seeded into 6-well plates. Till the cells reached 100% confluency, scratch was made in the plate using a P200 pipette tip. Images were collected at 0 h and 12 h under inverted microscope.

Cell invasion assay

Matrigel assay was performed using Transwell chambers (8 μm pore size, Millipore) that were pre-coated with 1 mg/ml Matrigel (Corning), and 5×10^4 cells were plated in the upper chamber of the Matrigel-coated Transwell insert. Cells were incubated for 12 h and cells remaining on the upper membrane were carefully removed. All cells were fixed cells in methanol and stained with crystal violet. Then the cells were counted under an inverted microscope.

TOP/FOP flash assay

To assess the transcriptional activity of β-catenin, A-498 cells grown in 24-well culture plates were transiently transfected with the 0.2 μg TOP flash (Promega) or the negative control FOP flash. 0.2 μg Renilla reporter luciferase plasmid was added as well. The luciferase activity was determined using a luciferase assay system (Promega) according to the manufacturer's specifications. Renilla activity was used to normalize for transfection efficiency.

Luciferase reporter assay

The 3′-UTR of wild type/mutant MAGI1 and MIR-520H promoter were synthesized by Sangon Biotech (Shanghai, China) and inserted into pGL3 luciferase reporter vector (Promega). phRL-TK Renilla luciferase reporter was used for luciferase assay normalization. 293T or A-498 cells were transfected with 50 ng wild-type or mutant luciferase reporters and miR-520h mimics/miR-NC and pcDNA3.1-c-Myb/pcDNA3.1, along with 10 ng Renilla luciferase vector with the PEIpro (Polyplus) reagent, respectively. After 48 h, luciferase activity was detected by the Dual-luciferase Reporter Assay System (Promega) and relative luciferase activity was normalized to Renilla luciferase activity.

Statistical analysis

All data were presented as mean ± SD values or Min to Max values using the GraphPad Prism software 7.0. The significance of differences between two groups was determined using a two-sided Student's *t* test. In case of multiple tests, one-way ANOVA followed by Bonferroni-Holm procedure was applied. Correlation was performed using two-tailed Spearman's test. $P \leq 0.05$ was considered statistically significant.

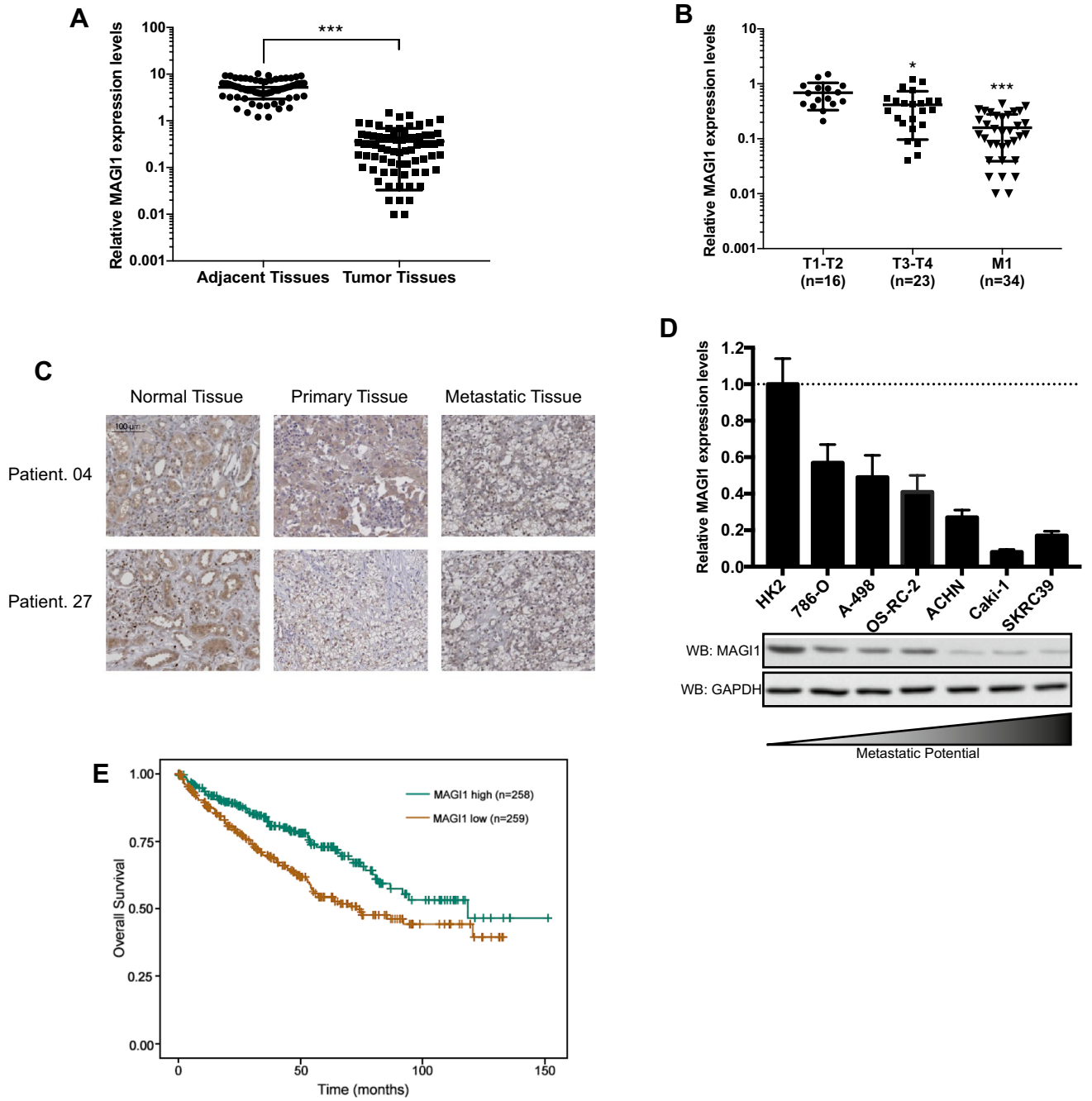

Fig. 1 The expression of MAGI1 is decreased in RCC and correlates with clinical outcome. **a** Relative MAGI1 expression in 73 paired RCC tumor tissues and adjacent normal tissues via qRT-PCR. **b** Relative MAGI1 expression of different T stages in RCC patients via qRT-PCR. **c** MAGI1 expression was examined by immunohistochemistry staining of different tissues in two paired RCC patients. **d** Relative MAGI1 expression in human renal cell lines via qRT-PCR (up) and western blot (down). **e** Kaplan–Meier analyses of the correlations between MAGI1 expression level and overall survival of 517 patients with RCC through TCGA analysis. Results are showed as mean ± SD of three independent experiments. *P < 0.05, ***P < 0.001

Results

MAGI1 is markedly decreased in metastatic RCC patients which indicates poor survival

We first examined the expression of MAGI1 in the 73 pairs of RCC tumor tissues and their corresponding adjacent normal kidney tissues by qRT-PCR. The results showed that MAGI1 expression was markedly decreased ($P < 0.001$) in the RCC tumor tissues when compared with adjacent non-cancerous kidney tissues (Fig. 1a). Moreover, MAGI1 expression in different tumor stages were analyzed. We found that MAGI1 expression was significantly lower in M1 stage than that in T1-T2 and T3-T4 stage RCC (Fig. 1b). To further investigate the correlation of MAGI1 expression with RCC clinicopathologic features, two paired specimens from normal, primary and metastatic tumor sites were subjected to immunohistochemical (IHC) staining with an antibody specifically against MAGI1. In line with qRT-PCR results, the expression level of MAGI1 was significantly reduced in tumor sites, especially in metastatic tumor sites, compared to normal adjacent non-cancerous kidney tissues (Fig. 1c). The observations above indicated a gradual loss of MAGI1 expression during the progression of RCC in clinic setting. To further ascertain the role of MAGI1, the expression of MAGI1 of several human RCC cell lines in mRNA level (up) and protein level (down) was examined. The results indicated that MAGI1 expression in RCC cell lines was lower than that in normal renal tubule epithelial cell line HK-2 and exhibited partly negative correlation with the metastatic ability of RCC cell lines (Fig. 1d). To validate the clinical significance of MAGI1 in RCC patients, a cohort of 517 clear-cell RCC (ccRCC) cases from the TCGA was analyzed. Kaplan–Meier survival analysis indicated that RCC patients with the lower levels of MAGI1 had shorter overall survival than those with the higher levels of MAGI1 (Fig. 1e, Log-Rank $P = 0.0014$). In all, our findings suggest that the expression of MAGI1 is decreased in RCC and its expression level is negatively associated with the progression of RCC.

MAGI1 mediates the invasion and migration of human RCC cells

In order to investigate the role of MAGI1 in RCC metastasis, we established MAGI1-overexpression and MAGI1-knockdown stable cell lines in A-498 and ACHN cells. The efficiency of MAGI1 overexpression and knockdown was confirmed at both protein and mRNA levels by western blot (left) and qRT-PCR (right), respectively

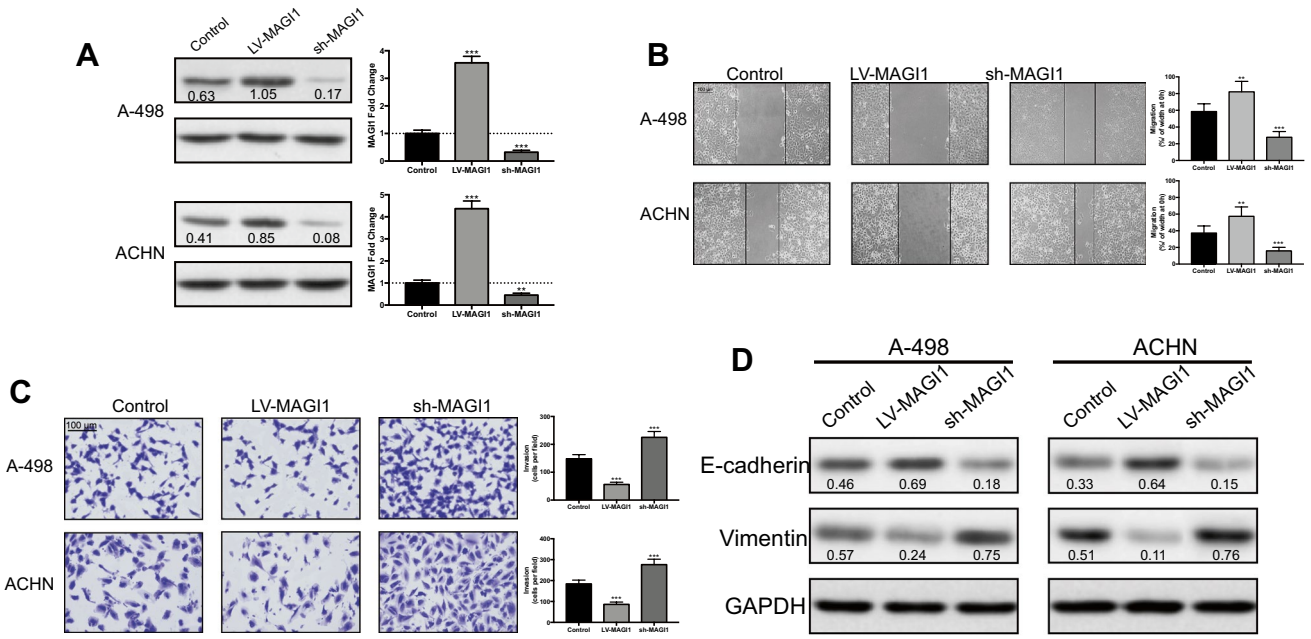

Fig. 2 MAGI1 expression level is correlated with RCC cell migration and invasion. **a** MAGI1 expression in constructed stable RCC cell lines were determined by western blot (left) and qRT-PCR (right). **b** The cell migratory ability of MAGI1-overexpression and MAGI1-knockdown cell lines were evaluated by wound healing assay; the wound healing assays were imaged at 12 h after scratches were made. **c** The cell invasive ability of MAGI1-overexpression and MAGI1-knockdown cell lines were performed by Transwell assay; the Transwell assays were imaged at 12 h after the cells be seeded. **d** MAGI1 expression modulated EMT markers in RCC cell lines. All bar graphs are plotted as mean ± S.D. P values are calculated between groups. $^{**}P < 0.01$; $^{***}P < 0.001$

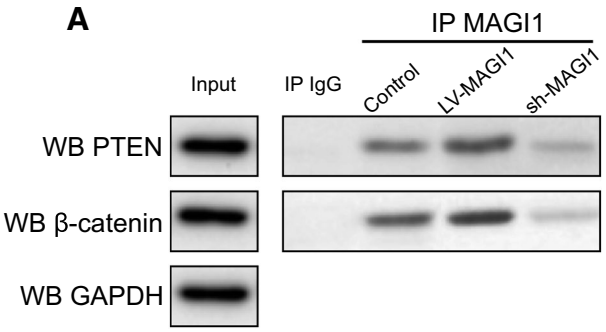
A
IP MAGI1
Input
IP IgG
Control
LV-MAGI1
sh-MAGI1
WB PTEN
WB β-catenin
WB GAPDH

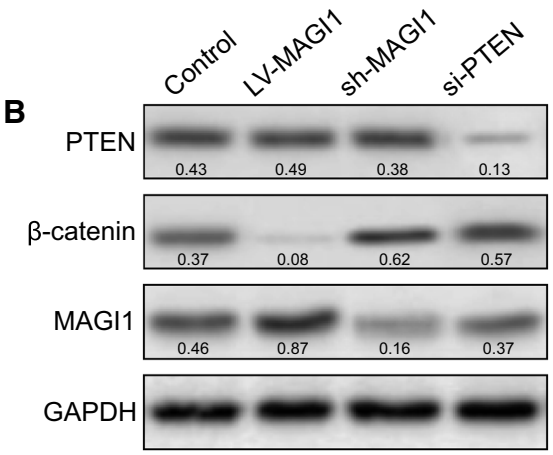
B
Control
LV-MAGI1
sh-MAGI1
si-PTEN
PTEN
0.43
0.49
0.38
0.13
β-catenin
0.37
0.08
0.62
0.57
MAGI1
0.46
0.87
0.16
0.37
GAPDH

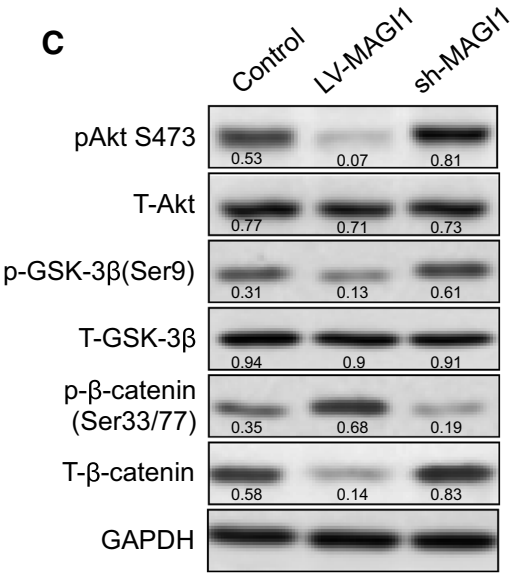
C
Control
LV-MAGI1
sh-MAGI1
pAkt S473
0.53
0.07
0.81
T-Akt
0.77
0.71
0.73
p-GSK-3β(Ser9)
0.31
0.13
0.61
T-GSK-3β
0.94
0.9
0.91
p-β-catenin (Ser33/77)
0.35
0.68
0.19
T-β-catenin
0.58
0.14
0.83
GAPDH

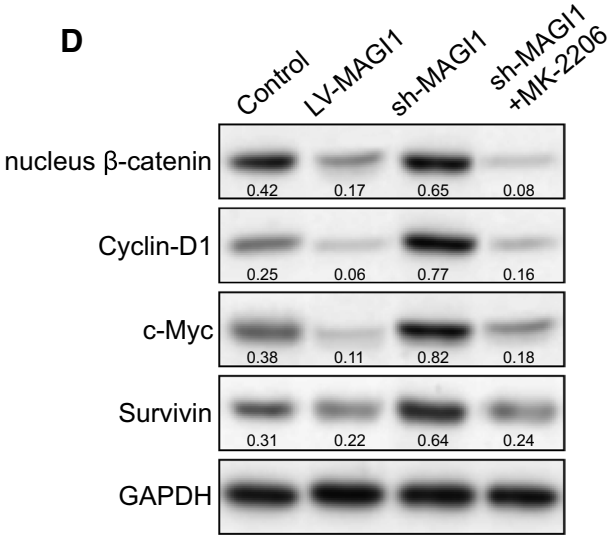
D
Control
LV-MAGI1
sh-MAGI1
sh-MAGI1 +MK-2206
nucleus β-catenin
0.42
0.17
0.65
0.08
Cyclin-D1
0.25
0.06
0.77
0.16
c-Myc
0.38
0.11
0.82
0.18
Survivin
0.31
0.22
0.64
0.24
GAPDH

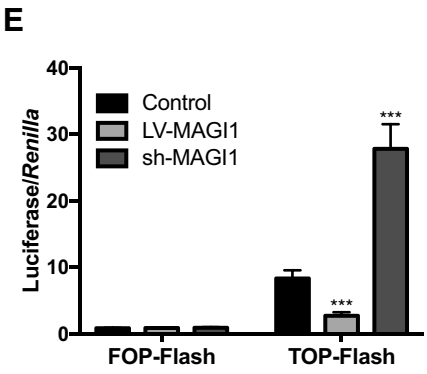
E
Luciferase/Renilla
40
30
20
10
0
Control
LV-MAGI1
sh-MAGI1
***
***
FOP-Flash
TOP-Flash

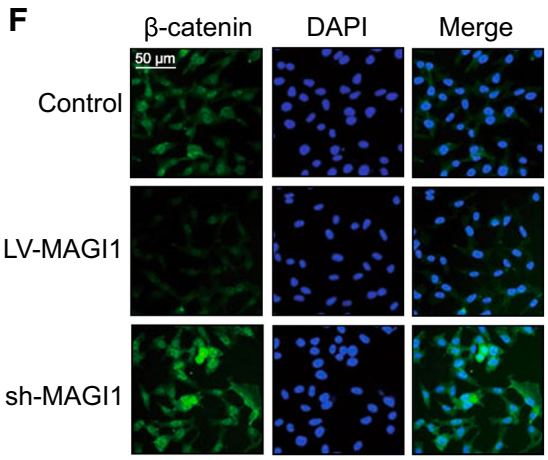
F
β-catenin
DAPI
Merge
50 μm
Control
LV-MAGI1
sh-MAGI1

◂**Fig. 3** MAGI1 recruits PTEN to inhibit β-catenin degradation in PTEN/MAGI1/β-catenin complex. **a** The PTEN/MAGI1/β-catenin complex was identified by co-immunoprecipitation. **b** β-catenin expression level was positively correlated with MAGI1 recruited PTEN. **c** MAGI1 modulated β-catenin expression level by regulating Akt/GSK-3β signaling. **d** MAGI1 regulated the β-catenin signaling pathway. **e** TOP/FOP Flash assay was performed to determine the activation of β-catenin signaling pathway. **f** the expression of β-catenin was assessed by immunofluorescence assay. ***$P < 0.001$

(Fig. 2a). Using wound healing assay, we examined the impact of overexpression and knockdown MAGI1 on RCC cell migration. We found that the migratory capacity of sh-MAGI1 cells was significantly increased compared to the control group (Fig. 2b, right). While the migratory capacity of LV-MAGI1 cells was remarkably decreased compared with the control cells (Fig. 2b, middle). To further examine the impact of MAGI1 on invasion, Matrigel-coated Transwell invasion assay was performed. Consistently, knockdown of MAGI1 promoted cell invasion, whereas overexpression of MAGI1 reduced invasive potential (Fig. 2c). In addition, the expression levels of EMT markers were examined by western blot. As shown in Fig. 2d, the expression of E-cadherin was downregulated, while the expression of Vimentin was dramatically increased in MAGI1-knockdown RCC cells. As expected, overexpression of MAGI1 increased the E-cadherin, but reduced the Vimentin expression. Thus, the MAGI1 expression level significantly influences the invasion and migration of human RCC cells.

MAGI1 stabilizes the PTEN/MAGI1/β-catenin complex to inhibit β-catenin signaling pathway

To further explore the underlying molecular mechanism of MAGI1-mediated RCC EMT, we first conducted IP studies in A-498 cells to confirmed whether MAGI1 functioned as a scaffolding molecule by recruiting PDZ (PSD-95/Dlg-A/ZO-1) domain binding proteins like phosphatase and tensin homolog deleted on chromosome ten (PTEN) and β-catenin as previously reported [14]. As shown in Fig. 3a, both PTEN and β-catenin bound with MAGI1 and varied in accordance with the amount of MAGI1. As activation of the Wnt/β-catenin signal pathway is one of most frequently involved in the initiation and progression of RCC [15], we detected the expression of β-catenin (Fig. 3b). The western blot results showed that β-catenin was negatively correlated with MAGI1, while PTEN remained unchanged. However, knockdown of PTEN significantly increased the expression of β-catenin. From these results, we hypothesized that MAGI1 functioned as a scaffolding protein to recruit PTEN and β-catenin to form a PTEN/MAGI1/β-catenin complex, in which PTEN promoted β-catenin degradation. To validate this hypothesis, we examined the key proteins regulating Akt/GSK-3β pathway that may be a link between PTEN and β-catenin. The results suggested that knockdown of MAGI1 increased Akt phosphorylation at Ser473 (active form), GSK-3β phosphorylation (inactive form) at Ser9 and decreased β-catenin phosphorylation at Ser33/77 (degradation form), which resulted in upregulation of total β-catenin (Fig. 3c). In contrast, MAGI1 overexpression did the opposite. Former studies have identified that activation of AKT could inhibit GSK3β kinase activity via phosphorylation of Ser9, which in turn decreased β-catenin phosphorylation and activated β-catenin pathway [16–18]. Moreover, knockdown of MAGI1 facilitated the nuclear translocation of β-catenin as determined by western blot (Fig. 3d) and immunofluorescence assays (Fig. 3f). Western blot (Fig. 3d) and TOP/FOP-Flash luciferase reporter analysis (Fig. 3e) revealed that knockdown of MAGI1 activated the β-catenin downstream signaling pathway. Conversely, overexpression of MAGI1 downregulated the β-catenin signaling pathway. Collectively, MAGI1 modulates β-catenin signaling pathway by stabilizing the PTEN/MAGI1/β-catenin complex in RCC.

MAGI1 is targeted by miR-520h

To further dissect the mechanism underlying MAGI1 modulating RCC metastasis, we searched for potential upstream regulator of MAGI1. Previous studies have demonstrated that common signaling pathways activate EMT regulators, which are also regulated by key microRNAs (miRNAs) [19]. Therefore, we screened 20 miRNAs that potentially targeted MAGI1 from three miRNA target-predicting algorithms including starBase, TargetScan and miRWalk (Fig. 4a), in which we focused on miR-520h that has been identified as upregulated miRNA correlated with metastasis progression of RCC (data from GSE23690, Table S2). Besides, qRT-PCR confirmed negative correlation between MAGI1 and miR-520h expression in RCC tumor specimens (Fig. 4b, $r = -0.711$, $P < 0.001$). By computational prediction of starBase, we identified the putative binding site of miR-520h with MAGI1 (Fig. 4c). Luciferase reporter assay demonstrated that miR-520h mimics markedly decreased the luciferase with the wild type 3′-UTR of MAGI1 mRNA in a dose dependent manner compared to that of mutant 3′-UTR of MAGI1 mRNA (Fig. 4d). Western blot confirmed that miR-520h mimics significantly decreased MAGI1 protein level in RCC cell lines as well (Fig. 4e). What's more, miR-520h mimics notably increased β-catenin expression and EMT markers (Fig. 4f). In brief, the data above reveal that MAGI1 is directly targeted by miR-520h in RCC cells.

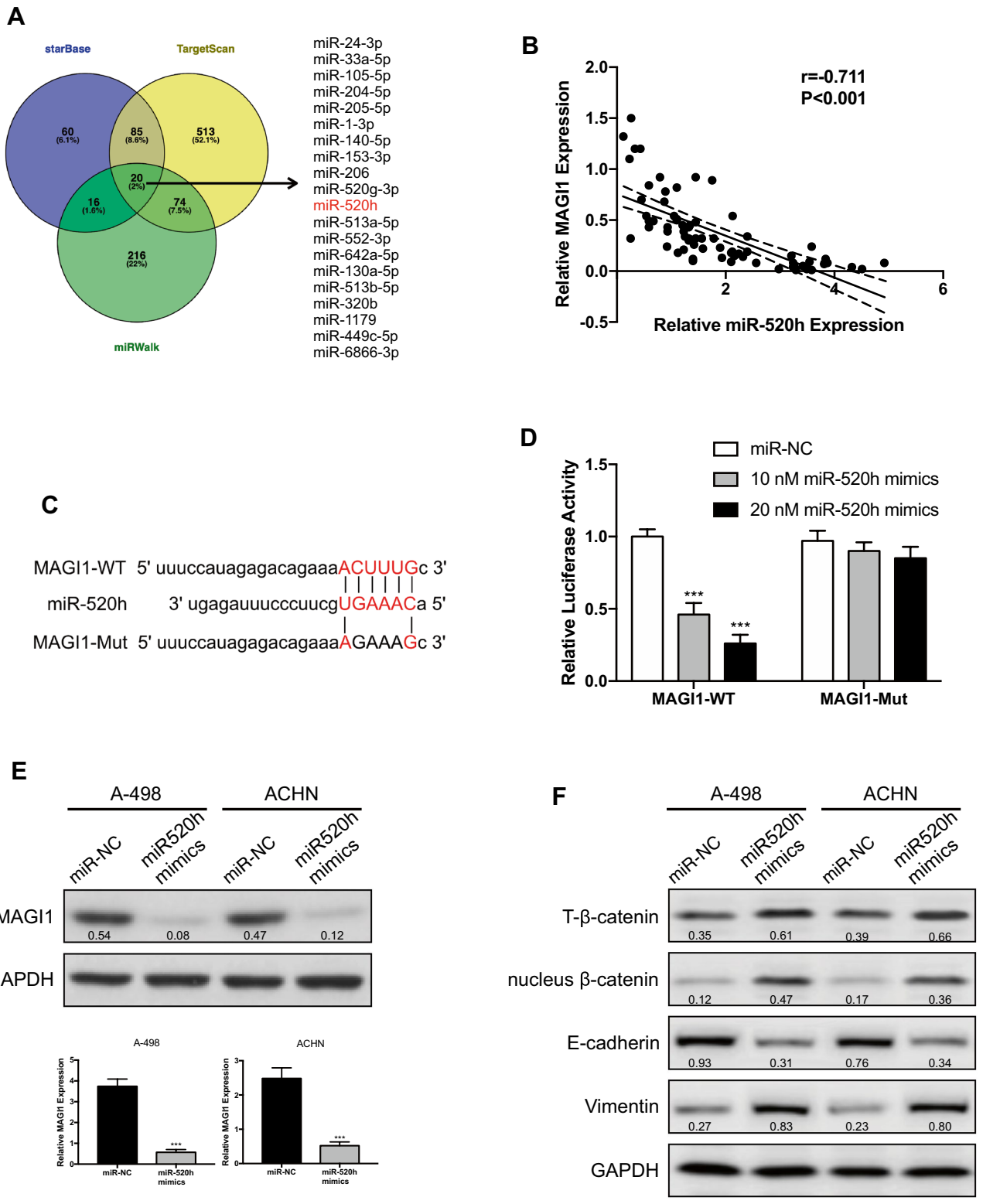

Fig. 4 MAGI1 is targeted by miR-520h. **a** Bioinformatics prediction of putative upstream miRNA targets of MAGI1 in three databases. **b** The correlation between miR-520h expression and MAGI1 expression in RCC patients' tumor specimen (n = 73). **c** The schematic illustration of predicted binding sites of miR-520h with the wild type and mutated 3′-UTR of MAGI1 mRNA. **d** Luciferase reporter assay of wild type and mutated 3′-UTR of MAGI1 mRNA in 293T cells. **e** Forced expression of miR-520h decreased the expression of MAGI1 in protein level (up) and mRNA level (down). **f** Forced expression of miR-520h increased β-catenin and EMT marker expression. Data shown are mean ± S.D. ***P < 0.001

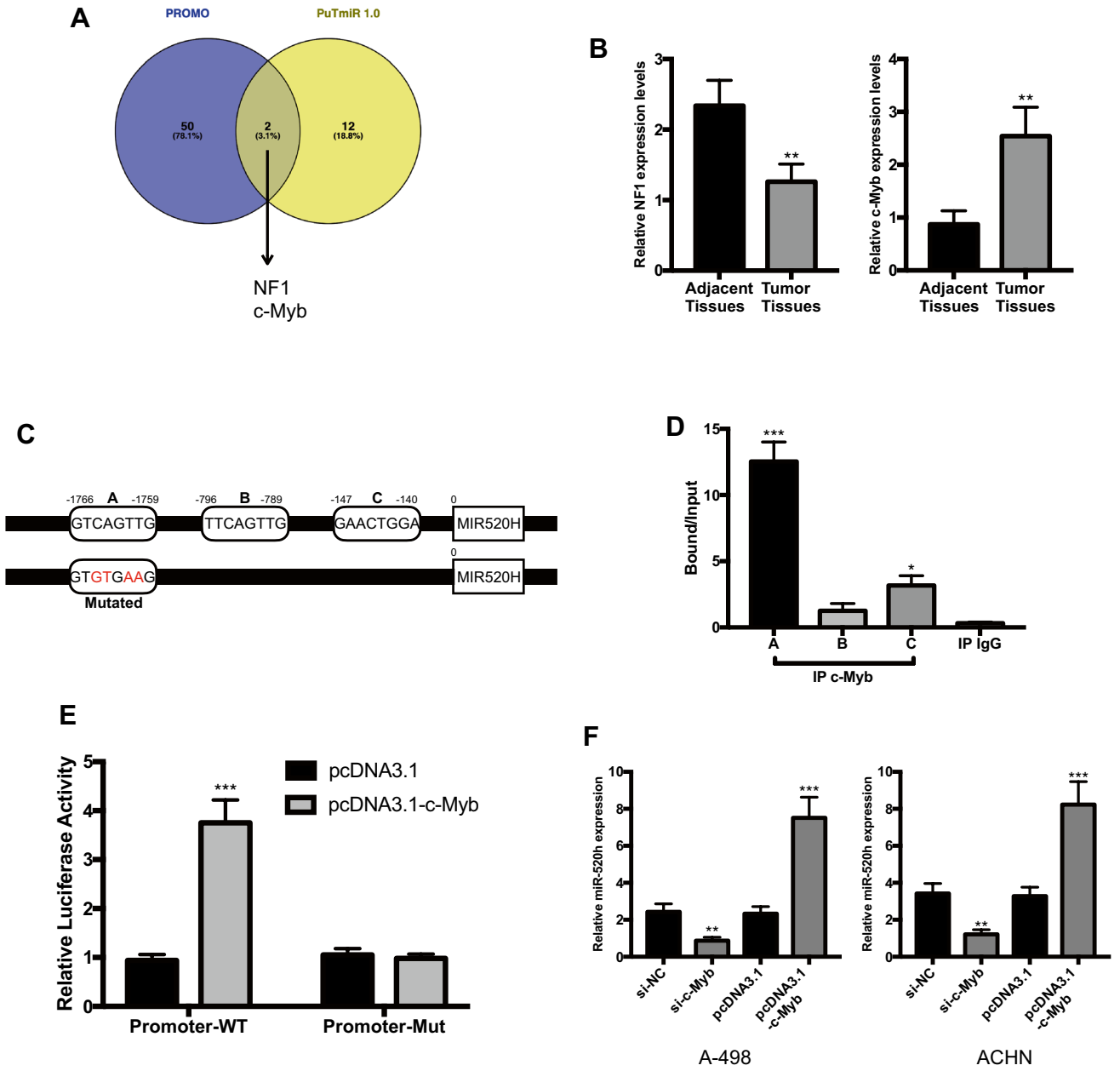

Fig. 5 c-Myb promotes the transcriptional activity of MIR-520H by binding with its promoter. **a** Bioinformatics prediction of putative upstream transcriptional factors of MIR-520H. **b** Relative expression of NF1 and c-Myb in 73 paired RCC tumor tissues and adjacent normal tissues via qRT-PCR. **c** Bioinformatics analysis of potential c-Myb binding sites in MIR-520H promoter. **d** Relative amount of indicated binding sites in the immunoprecipitates against c-Myb. **e** Luciferase reporter assays of wild type and mutated MIR-520H promoter in A-498 cells. **f** knockdown and overexpression of c-Myb affected the miR-520h expression

c-Myb promotes the transcriptional activity of MIR-520H by binding with its promoter

To investigate the mechanism responsible for the upregulation of miR-520h in RCC, we predicted 2 potential transcription factors, involving Neurofibromin 1(NF1) and c-Myb, in the promoter region of MIR-520H using PROMO and PuTmiR 1.0 (Fig. 5a). Then, the expression of NF1 and c-Myb in RCC tumor tissues and corresponding adjacent normal kidney tissues was determined by qRT-PCR. As showed in Fig. 5b, NF1 expression was lower in tumor tissues, while c-Myb expression was higher than normal tissues. Hence, we predicated the three-putative c-Myb binding sites (MBS) with MIR-520H promoter by PROMO (Fig. 5c).

Chromatin immunoprecipitation (ChIP) assay revealed that c-Myb was most significantly bound to MBS-A within the MIR-520H promoter (Fig. 5d). Luciferase assay also confirmed that c-Myb increased MIR-520H promoter activity, while this tendency was abolished in 520H promoter-mutant A-498 cells (Fig. 5e). Furthermore, qRT-PCR revealed that knockdown of c-Myb decreased miR-520h expression, but overexpression of c-Myb increased miR-520h expression (Fig. 5f). Taken together, these results above indicate that c-Myb promotes the transcriptional activity of MIR-520H by binding with its promoter in RCC.

Discussion

Metastasis are common found at diagnose and patients treated with nephrectomy in RCC [20]. However, the biomarkers and underlying mechanisms involving RCC metastasis remain elusive. These emphasize the urgent need to explore new biomarkers related to RCC metastasis. For the first time, this study demonstrated the role of MAGI1 on metastasis and its underlying mechanism in RCC. The results of this study suggest MAGI1 functions as tumor suppressor in RCC. Downregulation of MAGI1 decreases recruitment of PTEN to reduce β-catenin level in PTEN/MAGI1/β-catenin complex and activates β-catenin downstream signaling pathway, leading to increased invasion and migration of human RCC cells.

Previous studies have shown that PDZ domain-containing proteins, including MAGI1, were crucial on cellular adhesion and differentiation in mice [21]. MAGI1 downregulation were reported to be involved in migration and invasion of hepatocellular carcinoma, gastric cancer and colorectal cancer [11–13]. MAGI1 consists of six PDZ domains, a single catalytically inactive guanylate kinase domain and two WW (tryptophan–tryptophan) domains [22]. PDZ domains are docking domains for PDZ-binding molecules, whereby MAGI1 functions as a scaffolding molecule and associates with a variety molecules [23]. Larissa et al. have showed that PTEN and β-catenin could bind to the second and the fifth PDZ domain of MAGI1, respectively [14]. PTEN is a tumor suppressor gene, whereas β-catenin is widely known to promote tumor stemness and invasion. However, PETN knockdown could activate β-catenin signaling pathway via Akt/GSK-3β and promote cell invasion and migration in human gastric cancer [24]. Lu et al. have reported that disruption of adherens junctions could release β-catenin from the adherens junction complex, making it available for nuclear import and increased transactivation of β-catenin-responsive genes [25]. It is well known that Wnt/β-catenin signaling in human cancer is highlighted by its coordinate control of the transcriptional programs underlying EMT and cancer progression [26]. Moreover, prevention of β-catenin translocation from cell junctions to nucleus inhibited metastasis [27]. The results of our study demonstrated that the PDZ domain of MAGI1 recruited PETN and β-catenin, in which PETN mediated β-catenin degradation via Akt/GSK-3β as well. Thus, downregulation of MAGI1 may breakdown PETN/MAGI1/β-catenin complex and release β-catenin to enter the nucleus, leading to activated β-catenin signaling pathway and RCC metastasis.

MicroRNAs (miRNAs) are key regulators of gene expression, which post-transcriptionally repress gene expression by pairing to mRNAs [28]. Existing data have showed miRNAs can control metastasis through divergent or convergent regulation of metastatic gene pathways [29]. miR-520h, one member of the miR-520 family, has been reported to promote differentiation of HSCs into progenitor cells by inhibiting ABCG2 expression [30]. Nevertheless, the role of miR-520h in cancers may be cancer type dependent. Highly expressed miR-520h enhanced proliferation, migration and invasion in epithelial ovarian cancer and was associated with poor prognosis and lymph node metastasis in human breast cancer [31, 32]. On the other hand, introduction of miR-520h mimics into pancreatic cancer cells resulted in inhibition of cell migration and invasion [33]. Interestingly, miR-520c-3p, belongs to the miR-520 family as well, inhibited renal carcinoma cell growth, invasion, and migration by suppressing SPOP [34]. This study reveals that miR-520h functions as an oncomiRNA in RCC progression.

The transcription factor c-Myb has been identified as an oncogene that is involved in leukemia, colon cancer and breast cancer [35]. Li et al. identified that c-Myb enhanced breast cancer invasion and metastasis through interacting with β-catenin directly [36]. While Chen et al. reported that c-Myb promoted the invasion of hepatocellular carcinoma via increasing the transcription activity of osteopontin indirectly [37]. Except for collaborating with protein-encoding promoter, c-Myb also enhanced long non-coding RNA SNHG10 promoter activity to facilitate hepatocarcinogenesis and metastasis [38]. In the present study, we demonstrate that c-Myb is upregulated in RCC tissues and induces MIR-520H promoter activity.

In summary, this study demonstrates that MAGI1 is markedly decreased in mRCC comparing to adjacent normal tissues and low stage tumors. Overexpression or knockdown of MAGI1 significantly affects invasion and migration of human RCC cells via modulating PETN/MAGI1/β-catenin complex. In addition, c-Myb could bind with MIR-520H promoter and increase its expression. In turn, upregulated miR-520h directly targets MAGI1 to downregulate MAGI1 expression. Our findings suggest MAGI1 as a novel mediator of RCC metastasis and may prove to be a clinically useful biomarker and target for developing new diagnose and treatment methods for RCC progression and metastasis.

Acknowledgements The work was supported by grant from the National Natural Science Foundation of China (Grant No. 21300005131323).

Author contributions WW and TZ conceived and designed the experiments; WW, YY and XC performed the experiments; WW, SS and SH analyzed the data; WW and TZ wrote the paper.

Compliance with ethical standards

Conflict of interest The authors confirm that there is no conflict of interest.

References

1. Bray F, Ferlay J, Soerjomataram I, Siegel RL, Torre LA, Jemal A (2018) Global cancer statistics 2018: GLOBOCAN estimates of incidence and mortality worldwide for 36 cancers in 185 countries. CA Cancer J Clin 68(6):394–424
2. Barata PC, Rini BI (2017) Treatment of renal cell carcinoma: current status and future directions. CA Cancer J Clin 67(6):507–524
3. Dabestani S, Thorstenson A, Lindblad P, Harmenberg U, Ljungberg B, Lundstam S (2016) Renal cell carcinoma recurrences and metastases in primary non-metastatic patients: a population-based study. World J Urol 34(8):1081–1086
4. Lalani AA, McGregor BA, Albiges L, Choueiri TK, Motzer R, Powles T et al (2019) Systemic treatment of metastatic clear cell renal cell carcinoma in 2018: current paradigms, use of immunotherapy, and future directions. Eur Urol 75(1):100–110
5. Hakimi AA, Voss MH, Kuo F, Sanchez A, Liu M, Nixon BG et al (2019) Transcriptomic profiling of the tumor microenvironment reveals distinct subgroups of clear cell renal cell cancer: data from a randomized phase III trial. Cancer Discov 9(4):510–525
6. Knights AJ, Funnell AP, Crossley M, Pearson RC (2012) Holding tight: cell junctions and cancer spread. Trends Cancer Res 8:861–869
7. Friedl P, Mayor R (2017) Tuning collective cell migration by cell-cell junction regulation. Cold Spring Harb Perspect Biol 9(4):a029199
8. Woodcock SA, Rooney C, Liontos M, Connolly Y, Zoumpourlis V, Whetton AD et al (2009) Src-induced disassembly of adherens junctions requires localized phosphorylation and degradation of the rac activator Tiam1. Mol Cell 33(5):639–653
9. Abe JI, Ko KA, Kotla S, Wang Y, Paez-Mayorga J, Shin IJ et al (2019) MAGI1 as a link between endothelial activation and ER stress drives atherosclerosis. JCI Insight 4(7):e125570
10. Feng X, Jia S, Martin TA, Jiang WG (2014) Regulation and involvement in cancer and pathological conditions of MAGI1, a tight junction protein. Anticancer Res 34(7):3251–3256
11. Zhang G, Wang Z (2011) MAGI1 inhibits cancer cell migration and invasion of hepatocellular carcinoma via regulating PTEN. Zhong Nan Da Xue Xue Bao Yi Xue Ban 36(5):381–385
12. Zaric J, Joseph JM, Tercier S, Sengstag T, Ponsonnet L, Delorenzi M et al (2012) Identification of MAGI1 as a tumor-suppressor protein induced by cyclooxygenase-2 inhibitors in colorectal cancer cells. Oncogene 31(1):48–59
13. Jia S, Lu J, Qu T, Feng Y, Wang X, Liu C et al (2017) MAGI1 inhibits migration and invasion via blocking MAPK/ERK signaling pathway in gastric cancer. Chin J Cancer Res 29(1):25–35
14. Kotelevets L, van Hengel J, Bruyneel E, Mareel M, van Roy F, Chastre E (2005) Implication of the MAGI-1b/PTEN signalosome in stabilization of adherens junctions and suppression of invasiveness. FASEB J 19(1):115–117
15. Wen JL, Wen XF, Li RB, Jin YC, Wang XL, Zhou L et al (2015) UBE3C promotes growth and metastasis of renal cell carcinoma via activating Wnt/beta-catenin pathway. PLoS ONE 10(2):e0115622
16. Buttrick GJ, Wakefield JG (2008) PI3-K and GSK-3: Akt-ing together with microtubules. Cell Cycle 7(17):2621–2625
17. Wu D, Pan W (2010) GSK3: a multifaceted kinase in Wnt signaling. Trends Biochem Sci 35(3):161–168
18. Zhou BP, Deng J, Xia W, Xu J, Li YM, Gunduz M et al (2004) Dual regulation of Snail by GSK-3beta-mediated phosphorylation in control of epithelial-mesenchymal transition. Nat Cell Biol 6(10):931–940
19. Mittal V (2018) Epithelial mesenchymal transition in tumor metastasis. Annu Rev Pathol 13:395–412
20. Choueiri TK, Motzer RJ (2017) Systemic therapy for metastatic renal-cell carcinoma. N Engl J Med 376(4):354–366
21. Nguyen MM, Nguyen ML, Caruana G, Bernstein A, Lambert PF, Griep AE (2003) Requirement of PDZ-containing proteins for cell cycle regulation and differentiation in the mouse lens epithelium. Mol Cell Biol 23(24):8970–8981
22. Ghimire K, Zaric J, Alday-Parejo B, Seebach J, Bousquenaud M, Stalin J et al (2019) MAGI1 mediates eNOS activation and NO production in endothelial cells in response to fluid shear stress. Cells 8(5):388
23. Sakurai A, Fukuhara S, Yamagishi A, Sako K, Kamioka Y, Masuda M et al (2006) MAGI-1 is required for Rap1 activation upon cell-cell contact and for enhancement of vascular endothelial cadherin-mediated cell adhesion. Mol Biol Cell 17(2):966–976
24. Ma J, Guo X, Zhang J, Wu D, Hu X, Li J et al (2017) PTEN gene induces cell invasion and migration via regulating AKT/GSK-3beta/beta-catenin signaling pathway in human gastric cancer. Dig Dis Sci 62(12):3415–3425
25. Lu Z, Ghosh S, Wang Z, Hunter T (2003) Downregulation of caveolin-1 function by EGF leads to the loss of E-cadherin, increased transcriptional activity of beta-catenin, and enhanced tumor cell invasion. Cancer Cell 4(6):499–515
26. Liu H, Yin J, Wang H, Jiang G, Deng M, Zhang G et al (2015) FOXO3a modulates WNT/beta-catenin signaling and suppresses epithelial-to-mesenchymal transition in prostate cancer cells. Cell Signal 27(3):510–518
27. Wang Y, Bu F, Royer C, Serres S, Larkin JR, Soto MS et al (2014) ASPP2 controls epithelial plasticity and inhibits metastasis through beta-catenin-dependent regulation of ZEB1. Nat Cell Biol 16(11):1092–1104
28. Gurtan AM, Sharp PA (2013) The role of miRNAs in regulating gene expression networks. J Mol Biol 425(19):3582–3600
29. Pencheva N, Tavazoie SF (2013) Control of metastatic progression by microRNA regulatory networks. Nat Cell Biol 15(6):546–554
30. Liao R, Sun J, Zhang L, Lou G, Chen M, Zhou D et al (2008) MicroRNAs play a role in the development of human hematopoietic stem cells. J Cell Biochem 104(3):805–817
31. Zhang J, Liu W, Shen F, Ma X, Liu X, Tian F et al (2018) The activation of microRNA-520h-associated TGF-beta1/c-Myb/Smad7 axis promotes epithelial ovarian cancer progression. Cell Death Dis 9(9):884
32. Su CM, Wang MY, Hong CC, Chen HA, Su YH, Wu CH et al (2016) miR-520h is crucial for DAPK2 regulation and breast cancer progression. Oncogene 35(9):1134–1142
33. Wang F, Xue X, Wei J, An Y, Yao J, Cai H et al (2010) hsa-miR-520h downregulates ABCG2 in pancreatic cancer cells to inhibit migration, invasion, and side populations. Br J Cancer 103(4):567–574

34. Ding M, Lu X, Wang C, Zhao Q, Ge J, Xia Q et al (2018) The E2F1-miR-520/372/373-SPOP axis modulates progression of renal carcinoma. Cancer Res 78(24):6771–6784
35. Ramsay RG, Gonda TJ (2008) MYB function in normal and cancer cells. Nat Rev Cancer 8(7):523–534
36. Li Y, Jin K, van Pelt GW, van Dam H, Yu X, Mesker WE et al (2016) c-Myb enhances breast cancer Invasion and metastasis through the Wnt/beta-Catenin/Axin2 pathway. Cancer Res 76(11):3364–3375
37. Chen RX, Xia YH, Xue TC, Ye SL (2010) Transcription factor c-Myb promotes the invasion of hepatocellular carcinoma cells via increasing osteopontin expression. J Exp Clin Cancer Res 29:172
38. Lan T, Yuan K, Yan X, Xu L, Liao H, Hao X et al (2019) LncRNA SNHG10 facilitates hepatocarcinogenesis and metastasis by modulating its homolog SCARNA13 via a positive feedback loop. Cancer Res. https://doi.org/10.1158/0008-5472.can-18-4044